



Design and numerical analysis of a horizontal axis wind turbine

Shrayas Pradhan* and Sailesh Chitrakar

Department of Mechanical Engineering, Kathmandu University, Dhulikhel, Nepal.

Abstract

In this paper, mathematical design of a 20 kW horizontal axis wind turbine is conducted along with computational analysis to verify the performance of the designed blade. Blade Element Momentum (BEM) theory is used for the design of blades, empirical BEM relations for geometry calculations for twist distribution and chord distribution are included. The computational analysis on the performance of the geometric design is done using both BEM and Computational Fluid Dynamics (CFD) through Qblade BEM code and ANSYS CFX tool respectively. The rotational periodicity based domain is used for CFD computation and $k - \epsilon$ turbulence model is considered. The analysis is done in variable speed conditions (constant tip speed ratio of 6) for wind speed range 2-12 m/s, and change of pitch angles from 1 to 4°. The optimum pitch is obtained as 3° from CFD analysis. The results of torque, Cp/Power, velocity streamlines, and pressure contours are obtained from CFD. Torque curve obtained from BEM and CFD analysis over wind speeds 2-12 m/s showed good agreement, supporting the HAWT geometric design. A maximum Cp of 0.399 was obtained at 12 m/s.

Keywords: Horizontal Axis Wind Turbine (HAWT); Blade design; Blade Element Momentum Theory (BEM); Computational Fluid Dynamics (CFD); Performance analysis

1. Introduction

Small horizontal axis wind turbines up to 50 kW power generation capacities can be implemented in rural communities where the national electricity grid is inaccessible. A 3-bladed small scale HAWT of fixed pitch and variable speed is one of the most common wind turbines to be extensively used because of its simplicity, ease of manufacture, reliability, and relatively low cost. However, the design of small wind turbines needs to be verified computationally, so as to estimate the performance in different conditions.

The BEM approach is the most popular approach for wind turbine design and performance estimation in engineering. BEM theory is a validated and supported approach for the design of the wind turbine blades. It was developed as an extension of the Gaulert propeller theory. It discretizes the blade into several annular elements and assumes no radial interaction to predict parameters in each segment, then predicting the loads and power outputs from calculated or extrapolated 2D aerodynamic coefficients. The BEM approach can be implemented to design the rotor, the rotor design parameters such as rotor diameter, airfoils, chordal distribution, twist distribution, and evaluate the performance of the wind turbine at different wind conditions through the forces on the wind turbine blade, torque and power obtained. Although BEM has limitations, such that the fixed aerodynamic coefficients for airfoils are used, which does not match for all sections of blade, and detailed flow characteristics affecting performance cannot be considered, BEM is a good approximation to find the performance characteristics [1,2,3]. It can be observed from literature that the open-source BEM framework, Qblade has been used for the BEM design and BEM performance analysis of the wind turbine blade [4].

To support the BEM-based blade design, CFD is a complementary approach to support the BEM design. It is based on the discretization of control volumes and the finite volume method. It is an ideal

approach for investigating the complex flows in a wind turbine blade, including the radial flows, not considered by BEM theory. The CFD approach also provides a detailed analysis of the blade surface including the blade surface pressure distributions, blade velocity streamlines, and near velocity fields. However, CFD is a computationally intense approach and is seldom used as an optimization tool, but it can still be used to verify the BEM design. CFD using commercial CFD software have utilized different turbulence models such as $k - \omega$ SST, standard $k - \omega$ models, and results experimentally validated [5,6,7,8]. This paper focuses on the design and numerical performance investigation of a 20 kW, 3 bladed, up-wind fixed pitch variable speed small scale wind turbine, delving into the detailed geometric design utilizing the Blade Element Momentum (BEM) theory, and numerical investigations into the performance characteristics of the designed blade using both Computational Fluid Dynamics (CFD) and BEM theory. In the paper, a periodicity based domain setup and $k - \epsilon$ turbulence model was considered for the CFD analysis over different pitch angles and wind velocities from 2-12 m/s.

2. Method

2.1. BEM design of wind turbine

The BEM approach is used for the geometric design and performance analysis of the wind turbine. The BEM theory is a combination of the Blade element theory and the momentum theory, which can be applied to obtain the forces and torque acting on the wind turbine blade, and the corresponding power [9].

Fig. 1 shows the forces acting on the wind turbine blade section, normal force (dN), tangential torque (dT), lift force (dL), drag force (dD), the angle of relative wind (ϕ), consisting of twist angle (θ) and angle of attack (α), and axial (a) and tangential (a') induction factor. Ω is the radial velocity of the blade section and r is the sectional length of the wind turbine blade. V_{rel} is the relative velocity and

*Corresponding author. Email: shrayas.pradhan@gmail.com

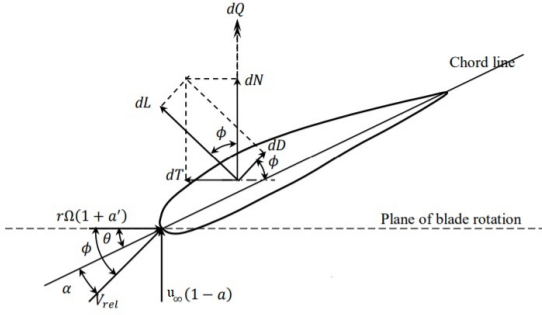


Figure 1: Forces acting on annular section of wind turbine blade.

u_∞ is the free stream velocity.

The normal force dN and torque dT is given by equation 1 and 2. The forces can be integrated over the entire section of wind turbine blade to obtain total force and torque, and the corresponding power.

$$dN = \frac{\rho [(1-a)u_\infty]^2}{2 \sin^2 \phi} B (C_L \cos \phi + C_D \sin \phi) c dr \quad (1)$$

$$dQ = \frac{\rho (1-a) u_\infty}{2 \sin \phi} \frac{(1+a') \omega r}{\cos \phi} B (C_L \cos \phi + C_D \sin \phi) c dr \quad (2)$$

C_L and C_D are the coefficient of lift and drag respectively, depending on the Reynolds number, the angle of attack and the selection of airfoil for the section. The aerodynamic coefficients of the different thicknesses of s822 and s823 airfoils for high angle of attacks were obtained by extrapolation in XFOIL available in the Qblade tool [4].

To evaluate the torque and the normal force, the tangential and axial induction factors are solved iteratively. The equations of axial and tangential induction factors are given in equation 3 and 4, and are obtained by the conservation of momentum in the axial direction from the upstream and downstream section [9].

$$a = \frac{1}{\frac{4F \sin^2 \phi}{\sigma (C_L \cos \phi + C_D \sin \phi)} + 1} \quad (3)$$

$$a' = \frac{1}{\frac{4F \sin \phi \cos \phi}{\sigma (C_L \sin \phi - C_D \cos \phi)} + 1} \quad (4)$$

Where, F is the loss factor, is given by equation 5 [10].

$$F = \frac{2}{\pi} \cos^{-1} \left\{ \exp \left[-\frac{B(r-R)}{2r \sin \phi} \right] \right\} \cdot \frac{2}{\pi} \cos^{-1} \left\{ \exp \left[-\frac{B(1-\frac{r}{R})}{2\frac{r}{R} \sin \phi} \right] \right\} \quad (5)$$

And, σ is the solidity of the wind turbine, given by equation 6.

$$\sigma = \frac{BC}{2\pi r} \quad (6)$$

The Coefficient of power (C_P) of the wind turbine, from the BEM theory is then given by the equation 7.

$$C_p = \frac{P}{\frac{1}{2} \rho u_\infty^3 A} \quad (7)$$

For the geometric parameters, there are several parameters that need to be considered before the BEM geometric design, which are tabulated in Table 1.

Table 1: Design parameters of wind turbine.

Parameter	Value
Wind Turbine Rated Power (P)	20 kW
Control	Fixed Pitch- Variable speed (TSR at 6)
Wind Turbine rated/ design speed	12m/s
Air Density (ρ)	1.1839 kg/m ³
Assumed initial power coefficient (C_P)	0.3
Number of Blades (B)	3
TSR at design condition (λ)	6
Radius of Blade (R)	4.5 m
Rated Speed	150 RPM
Airfoils	S823 at root and transition, s822 at tip

For the BEM based geometric design, the length of the blade was discretised into 30 sections. The s823 and s822 airfoil family for small scale wind turbine up to 20 kW capacity was considered for the blade [11]. The twist angle of each section of the blade depends on the inflow angle of the section, which is expressed as a function of the tip speed ratio (λ) and is given by equation 8.

$$\phi = \left(\frac{2}{3} \right) \tan^{-1} \frac{1}{\lambda \left(\frac{r}{R} \right)} \quad (8)$$

The twist angle for each section depends on the inflow angle and the optimum angle of attack (α). The optimum angle of attack for the s823 and s822 airfoils are taken as 6.25° and 4.75° respectively. For high inflow angles of 70-80°, the aerodynamic coefficients are extrapolated from XFOIL to a full 360°, under the assumption that all airfoils behave like a thin flat plate in high angle of attack. The twist angle for each section is given by equation 9.

$$\theta = \phi - \alpha \quad (9)$$

From the BEM approach, different sections of the blade have different chordal distributions similar to the different inflow angles. The individual chords are inversely proportional to the local tip speed ratio, implying as the sectional radius of the blade decreases, the chord length increases accordingly, making the blade tapered. While the Betz chordal formula can be used to obtain chordal distribution, the optimized Betz and Schmitz optimized chord distribution formulas based on local tip speed ratio and C_L can be used to obtain chord lengths. It should be noted that the C_L is taken from the expected tip speed ratio and the inflow angle for individual elements. Betz and Schmitz chord optimization formulas can be used to calculate the chordal distribution of the blade and are expressed by the equations 10 and 11 respectively [12]. The optimized Schmitz chordal distribution was considered for the BEM based design.

Betz chord optimization equation:

$$c(r) = \frac{16}{9} \frac{\pi R}{BC_L \lambda \frac{r}{R}} \frac{1}{\sqrt{\lambda \frac{r}{R} \frac{r}{R} + \frac{4}{9}}} \quad (10)$$

Schmitz chord length optimization formula:

$$c(r) = \frac{16\pi r}{BC_L} \sin^2 \left(\frac{1}{3} \tan^{-1} \left(\lambda \frac{r}{R} \right) \right) \quad (11)$$

Fig. 2 shows the chordal distribution of the wind turbine blade, calculated from both Betz and Schmitz optimization formulas, and the twist distribution for each section, for the wind turbine blade.

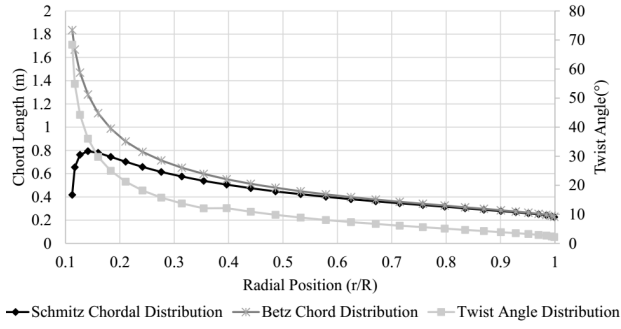


Figure 2: Chord and twist distribution of wind turbine blade.

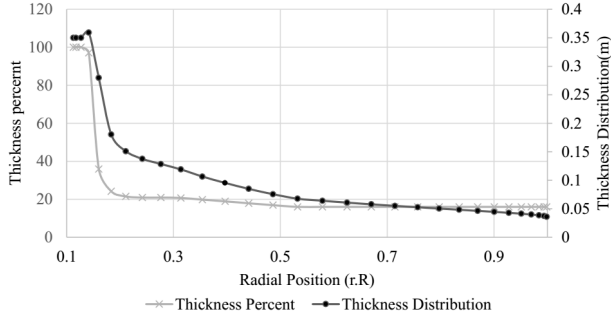


Figure 3: Thickness distribution of wind turbine blade.

In the paper, the thickness distribution of the wind turbine blade is considered. Although it is preferable to use the standard airfoils throughout the entire length of the wind turbine blade, in practice, different thickness of the airfoils are used in the wind turbine. In the blade design, two airfoils s823 for the root region and s822 airfoil for the tip region have been selected. In the transition between the airfoil, different thicknesses of the standard airfoils have been selected to ensure smooth transition between regions and ensure stiffness of the blade. In the bottom root region connecting to the hub, a circular airfoil has been selected. The twist, chord, thickness and airfoil distribution of the airfoil, designed in CAD software is illustrated in Fig. 3.

Fig. 4 shows the distribution of the blade profile and CAD model summarizing all the geometric parameters of wind turbine blade design, including twist, chord, thickness and airfoil distribution.

2.2. Numerical simulations using CFD

CFD includes the combined solutions of fundamental fluid flow equation and Reynolds-averaged Navier-Stokes equation, consisting of set of partial differential equations in the integral form of mass, momentum and energy conservation, using certain turbu-

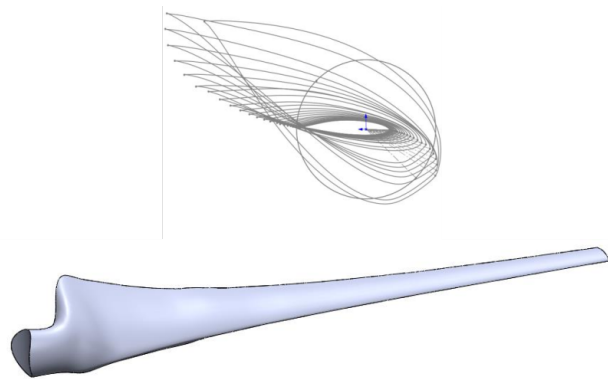


Figure 4: CAD model of the wind turbine blade.

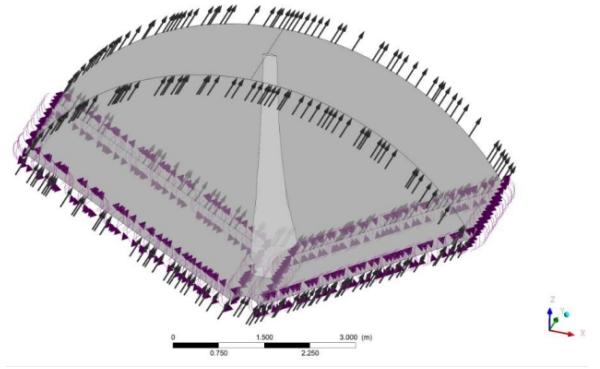


Figure 5: Rotational periodicity fluid domain and setup for CFD.

lence models to compute the average turbulence stress. These equations are then numerically solved over the specified domain, which consists of a rotational periodicity domain around a single blade. The continuity equation is given by equation 12.

$$\frac{\partial \rho}{\partial t} + \nabla \cdot (\rho U) = 0 \quad (12)$$

The RANS momentum equation is written as equation 13:

$$\frac{\partial \rho U}{\partial t} + \nabla \cdot (\rho U \otimes U) = -\nabla p + \nabla \cdot \left\{ \tau - \rho u \otimes u \right\} + S_M \quad (13)$$

Where, ρ is the density, τ is the stress factor, p is the static pressure and S_M is the sum of body forces.

The standard $k - \varepsilon$ turbulence model is used to solve the additional terms in the momentum equation by solving for two transport variables, turbulent kinetic energy (K) and the rate of dissipation of turbulent energy (ε). The $k - \varepsilon$ turbulence model is a robust and simple model to represent the turbulence variation, exhibiting excellent performance for many industrial flows. While the $k - \varepsilon$ turbulence model performs poorly for some unconfined flows, rotating flows, and non-circular ducts, it is validated to perform well for external flow problems around complex geometries such as wind turbine blades [13,14].

While the continuity equation remains the same for the $k - \varepsilon$ turbulence model, the change in the momentum equation is given in equation 14.

$$\frac{\partial \rho U}{\partial t} + \nabla \cdot (\rho U \otimes U) = -\nabla p' + \nabla \cdot \left\{ u_{\text{eff}} (\nabla U + (\nabla U)^T) \right\} + S_M \quad (14)$$

Where, u_{eff} is the effective viscosity that operates with the velocity gradients given by equation 15.

$$\mu_{\text{eff}} = \mu + \mu_t \quad (15)$$

Where, μ_t is the turbulence viscosity. The $k - \varepsilon$ turbulence model assumes the following relation between the turbulence viscosity, k , and ε .

$$\mu_t = C_\mu \rho \frac{k^2}{\varepsilon} \quad (16)$$

Where, C_μ is a constant.

In the computational domain, the hub, tower, nacelle and extreme tip of the wind turbine are neglected, which is an adequate approximation for performance simulation. The computational domain is a 120° rotational periodicity domain enclosing one blade. The fluid domain and its setup in ANSYS CFX, used for simulations is shown in Fig. 5.

Mesh generation is done to create a suitable numerical domain over the geometric feature in which the solver solves the required

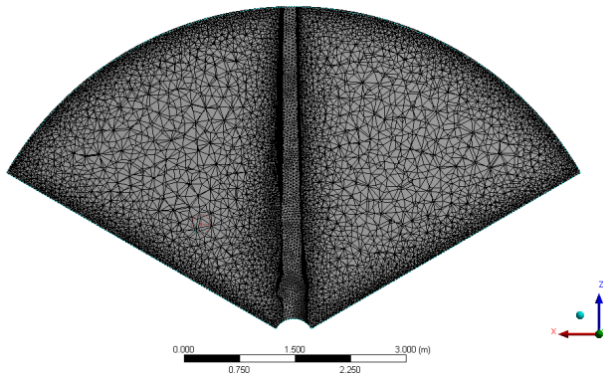


Figure 6: Mesh generation over domain.

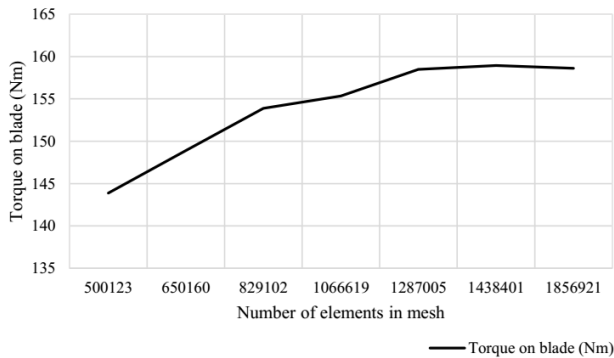


Figure 7: Mesh independence test.

equations. ANSYS Workbench was used for meshing. Meshing allows for the generation of structured and unstructured meshes. The physical preference for mesh generation was CFD and solver preference was CFX. Tetrahedral meshes have been used on the domain. The tetrahedral meshes are easy to resolve and the computational time necessary to solve such meshes are less compared to hexahedral and other meshes while providing satisfactory quality of the meshes. Inflation layer with layer quantity of 15 and growth rate 1.2 was taken in the domain surrounding the blade.

The solution obtained depends on the number of elements and the quality of mesh in the domain. A large number of elements with finer meshes predict the solution accurately at the expense of higher computational time. The number of elements in mesh was increased from 0.5 million to 1.8 million by increasing at a rate of 1.3. Fig. 7 shows the mesh independence test of the wind turbine blade at the inlet condition of 7 m/s. The torque reaches an asymptote beyond 1.2 million elements, which is the minimum elements necessary for an independent solution. All simulations were then carried out with more than 1.3 million elements in the domain.

The 3D Navier-Stokes CFD solver ANSYS CFX was used to compute the results over the domain. Steady-state fluid inlet of air from 2-12 m/s was taken in the inlet of the domain, and static pressure outlet of 1 atm was taken, with rotational velocity corresponding to 6 for particular inlet velocity. The CFX solver preferences, the solver parameters, the physical time-step was taken as 0.1s, convergence criteria of Root Mean Square (RMS) residual were taken as 1×10^{-4} , and a maximum of 100 iterations were taken to achieve the accurate results.

3. Results and discussion

3.1. CFD results

The results of the velocity streamlines, pressure distributions, and force calculations were obtained from ANSYS CFX post-

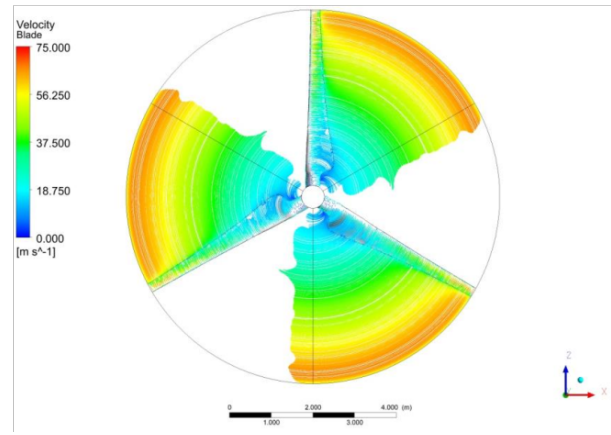


Figure 8: Relative velocity streamlines of blade at 12 m/s.

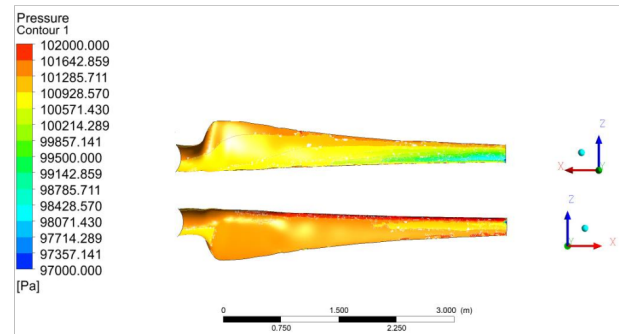


Figure 9: Pressure distribution on suction and pressure side of blade at 12 m/s.

processing. From the relative velocity streamlines of the blade at 12 m/s shown in Fig. 8, which corresponds to the tangential velocity of the turbine blade, it was noted that the CFD simulations also support the theoretical calculations such that the velocity developed corresponds to the tip speed ratio intended for the rotational velocity, among other computational indicators such as mass balance and residual criteria. From the pressure distribution. From Fig. 9, it can be seen that the pressure difference between the suction and pressure side of the rotor is high at the tip compared to the mid and root region of the rotor. The pressure difference at 12 m/s wind speed, qualitatively seen is responsible for the torque and the moments developed on the blade. The CFD simulation was carried out and similar results were obtained for all computations done on pitch angles varied from 1-4° for 8-12 m/s inlet velocity, and changing inlet velocity from 2-12 m/s for optimal pitch angle.

The CFD analysis of the wind turbine blade was done on same domain for various pitch angles to determine the optimum pitch angle for maximum power output. Power output in terms of torque of a single blade was done for 1°-4° pitch angles for high wind speeds 8-12 m/s. From the CFD analysis, it was observed that the pitch angle that produced the most torque output for the same boundary conditions was of 3° pitch. Since the wind turbine design considered is of FPVS type, the 3° pitch was selected and the subsequent CFD and BEM simulations were carried out. The Fig. 10 shows the variation of torque with different pitch angles at the same boundary condition CFD simulations.

3.2. Torque comparison from BEM and CFD

The CFD and BEM analysis of the wind turbine design over a wind speed range of 2-12 m/s at design tip speed ratio of 6 and pitch of 3° to yield the torque on the wind turbine blade as a characteristic variable. The torque results were obtained in post-processing

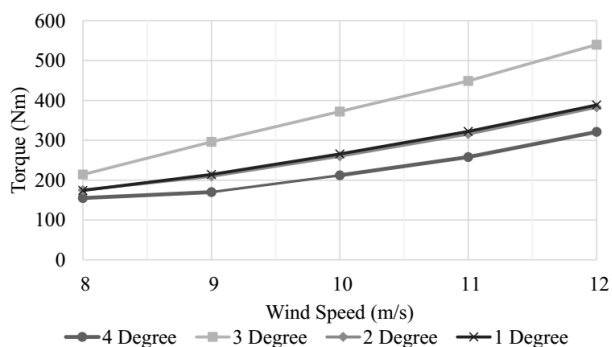


Figure 10: Pitch vs. torque.

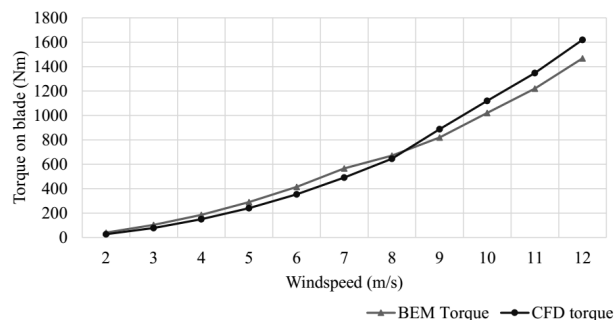


Figure 11: Torque vs. wind speed from BEM and CFD.

calculations of ANSYS CFX results and through the Qblade BEM simulations of the wind turbine. The results showed good agreement between torques from both BEM and CFD simulations, which is illustrated in Fig. 11. The difference in results could be attributed to the BEM approach of taking 2D aerodynamic coefficients and neglecting radial interaction among elements, which is distinct at higher wind speeds.

3.3. Power output with wind speed from CFD

The torque results obtained from CFD, along with the rotational speed of the blade at TSR of 6 at different wind speed, was used to calculate the power output of the wind turbine blade and is shown in Fig. 12. The coefficient of performance of the wind turbine blade at different wind speeds was also calculated. The maximum Cp of the wind turbine was found to be near 0.39 at wind speeds 9-12 m/s, which is stable compared to the increasing Cp of the wind turbine in the start-up phase at low wind speeds.

From the results, it can be inferred that 20 kW power is produced at wind speed of 11-12 m/s, with the wind turbine having a maximum coefficient of performance as 0.399 at 12 m/s. Thus, the presented data from both BEM and CFD is supportive of the wind turbine design based on the BEM theory as having a rated power of 20 kW.

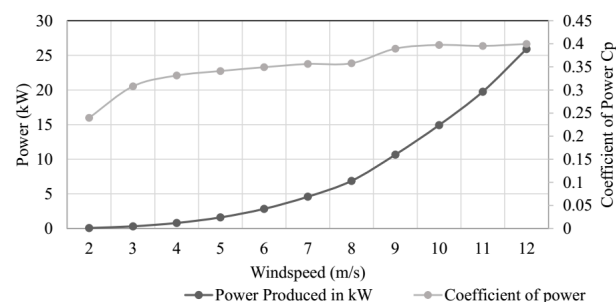


Figure 12: Power and Cp vs. wind speed from CFD.

4. Conclusion

The focus of the paper was towards the BEM design of the wind turbine and computational analysis of the designed wind turbine blade through BEM and CFD simulations. Initially, all input parameters of turbine design were calculated, and a geometric design of 20 kW FPVS HAWT was performed through the application of BEM theory. The NREL s822 and s823 airfoils were selected and the blade geometric parameters such as twist, chord and thickness distribution were calculated from the BEM approach. The design of the blades was subject to both BEM and CFD simulations in Qblade and ANSYS CFX respectively.

All CFD simulations were done with beyond 1.3 million elements in mesh after performing a mesh independent study. Parameters such as velocity, pressure contour, optimum pitch, torque, power, and Cp were obtained through CFD simulations over a wind speed range of 2-12 m/s for a constant TSR of 6. An optimum pitch angle of the blade as 3° was established through CFD simulations. The torque results, corresponding to power output were compared for both BEM and CFD simulations and showed good agreement in both results-providing support to the designed wind turbine blade. The maximum Cp of 0.399 was obtained over a wind speed range from 8-12 m/s.

References

- [1] Lanzafame R & Messina M, Fluid Dynamics Wind Turbine Design: Critical Analysis, Optimization and Application of BEM Theory, *Renewable Energy*, 32 (2007) 14 2291-2305.
- [2] Monteiro J, Silvestre M, Piggott H & Andre J C, Wind Tunnel Testing of a Horizontal Axis Wind Turbine Rotor and Comparison from Two Blade Element Momentum Codes, *Journal of Wind Engineering Industrial Aerodynamics*, 123 (2013) 99-106.
- [3] Yang H, Shen W, Xu H, Hong Z & Liu C, Prediction of the Wind Turbine Performance by Using BEM with Airfoil Data Extracted from CFD, *Renewable Energy*, 70(2014) 107-115.
- [4] Marten D & Wendler J, *Qblade Guidelines- v0.6*, Hermann Föttinger Institute, TU Berlin, Berlin, (2013).
- [5] Carcangiu C E, *CFD-RANS Study of Horizontal Axis Wind Turbines*, Ph. D. Thesis, Department of Mechanical Engineering, Università degli Studi di Cagliari, Spain, 2008.
- [6] Digraaskar D A, *Simulation of Flow Over Wind Turbines*, Masters Thesis, Department of Mechanical Engineering, University of Massachusetts Amherst, Massachusetts, USA, 2010.
- [7] Kim B, Kim W, Bae S, Park J & Kim M, Aerodynamic Design and Numerical Analysis of multi-MW class Wind Turbine Blade, *Journal of Mechanical Science and Technology*, 25 (2011) 1995-2002.
- [8] Bai C J, Hsiao F B, Li M H & Huang G Y, Design of 10 kW Horizontal Axis Wind Turbine Blade and Aerodynamic Investigation using Numerical Simulation, *Procedia Engineering*, 67 (2013) 279-287.
- [9] Hansen M O, *Aerodynamics of Wind Turbines*, Routledge Taylor and Francis Group, (1983), ISBN-13: 978-1844074389.
- [10] Manwell J F, McGowan J G & Rogers A L, *Wind Energy Explained, Theory, Design and Application*, John Wiley and Sons, (2009), ISBN-13: 978-0470015001.
- [11] Tangler J L & Somers D M, *NREL Airfoil Families for HAWTs*, National Renewable Energy Laboratory, U.S. Department of Energy, Golden, Colorado, USA, (1995).

- [12] Gasch R & Tvele J, *Wind Turbines: Basic Design, Planning and Operation*, Teubner, Wiesbaden, (2007).
- [13] Turbulent Flow Processes, *Process System Engineering*, 5 (2002) 57-83.
- [14] ANSYS Corporation, *CFD Theory and Models*, Canonsburg: ANSYS Corporation, (2012).